A Comparison between Directly Connected and MPPT Connected Solar Powered Water Pumping System using PMDC Motor

Partha Sarothi Sikder, Nitai Pal*

Department of Electrical Engineering, Indian Institute of Technology (Indian School of Mines), Dhanbad - 826004, India

Abstract

This paper represents a comparative analysis of two photovoltaic pumping systems. To study the performance of the Maximum Power Point Tracking (MPPT) system, two models were simulated using Matlab/Simulink and the performance of a directly connected photovoltaic (SPV) pumping system was compared to an MPPT connected SPV pumping system at various levels of solar irradiance. The MPPT system maximizes overall system efficiency, but makes the system complex compared to the directly connected SPV pumping system. Instead of the conventional boost converter the MPPT system contains a buck converter to maintain overall system voltage at the lower levels required by the permanent magnet DC (PMDC) motor. For simplicity, the MPPT controller follows the perturbation and observation (P & O) algorithm and controls the buck converter to maximize overall system efficiency at various levels of solar irradiance. The PMDC motor provides high weight-to-torque density, better speed control, low inertia, and lower losses compared to induction and the conventional DC motor. The comparative analysis shows that the MPPT connected SPV system is more efficient than the directly connected SPV system for water pumping purposes using a PMDC motor.

Keywords: Photovoltaic cell; MPPT; buck converter; PMDC motor; water pumping; modelling and simulation introduction

1. Introduction

In India most people live in rural areas and depend on agriculture, and access to reliable sources of water is a basic requirement for development. Ground water is preferable for drinking purposes, whereas surface water is widely used for agriculture and livestock purposes. The rural population faces a problem related to water for domestic and agricultural use, due to decreasing rainfall and uncertainty of the monsoon. Ground water levels are generally becoming lower and surface water is becoming scarcer. Often, it is not feasible or desirable to extract water using a traditional hand pump [1]. Traditional diesel or kerosene fueled engine pumps are commonly used for irrigation purposes, but they are costly in light of long-term rising fuel prices and are not environmentally friendly due to the emission of greenhouse gases and particulates which pollute the environment. Renewable energy sources are a desirable alternative for pumping water for drinking and agricultural purposes, without contaminating the environment. Wind energy is widely used worldwide for pumping water, but wind speeds in large parts of India are unsuitable for this task. Solar energy, however, is available.

Much research is going on to find suitable water pumping systems through SPV connected with DC and AC motors [2–8]. While the AC motor is less costly than the DC motor, the problem with the AC motor it that it is suitable for constant voltage operation, draws high current upon starting, is unstable at lower voltage [9] and requires an inverter for the SPV system, because SPV generates DC power [3, 4, 6]. The inverter adds extra cost and the lowers overall efficiency of the system. Compared to the AC motor, the DC motor provides good speed control, better torque at starting, good speed regulation and better efficiency [10]. But the conventional DC motor (separately excited and self excited) requires additional field supply, which complicates the system because SPV provides variable voltages dependent on fluctuating solar irradiance. The brushless DC motor is another alternative which provides good speed control, torque at starting, speed regulation and efficiency [8] but the problem related to the BLDC motor is cost and the power supply to the armature of the motor using hall sensor complicates the system and requires skilled operators for maintenance. Here an analysis is done using the PMDC motor, where the permanent magnet provides constant field excitation, the variable voltage of the SPV system supplies energy to the armature of the PMDC motor, and the motor rotates and provides speed

---

*Corresponding author
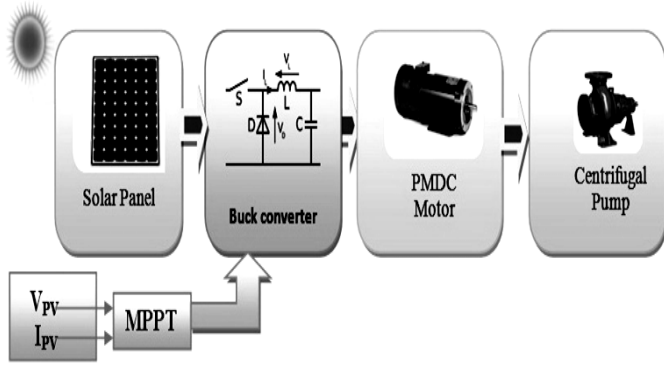*Email address:* `nitai_pal@rediffmail.com` (Nitai Pal)

Figure 1: MPPT connected SPV water pumping system using PMDC motor and centrifugal pump
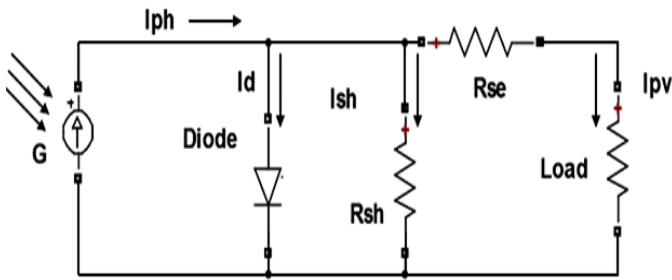

Figure 2: Equivalent circuit of SPV cell

by controlling the armature voltage from base speed to a reduced speed. As the I-V characteristic of the SPV system is nonlinear in nature, to utilize maximum power drawn from the SPV system a Maximum Power Point Tracking (MPPT) device is required, which follows an algorithm and increases the voltage level by changing the duty cycle of the DC-DC converter [11].

2. Configuration of the proposed system

A schematic diagram of the proposed system is shown in Fig. 1 where solar energy is converted into electricity which is DC in nature. The DC to DC converter is used to reduce the generated DC voltage by the buck converter using pulse width modulation (PWM) and the reduced voltage is applied to the PMDC motor according to the name plate data of the PMDC motor. The centrifugal pump is attached to the PMDC motor shaft. When sufficient electrical energy is generated by the solar panel, the motor starts rotating and the pump starts working. The MPPT technique follows an algorithm and increases the operating voltage level by changing the duty cycle of the DC-DC converter. Hence, maximum energy from the solar panel is utilized by the PMDC motor at various solar irradiance levels.

2.1. Photovoltaic system

Photovoltaic cells (PV) directly convert solar energy into electrical energy. A single PV cell produces a small amount of energy. To obtain a large amount of current and voltage

a large number of series parallel connection of PV cells is required. The equivalent circuit model and diagram is shown in Fig. 2. This consists of photon generated current, a diode, a parallel resistor preventing leakage current and a series resistor describing internal resistance of the cell [12, 13].

From the equivalent circuit shown in Fig. 2, applying Kirchhoff's current law PV cell equivalent circuit I_{PV} is found as shown in equation 1 [12–14].

$$I_{PV} = I_{ph} - I_d - I_{sh} \tag{1}$$

Here, I_{ph} represents the photon generated current, I_d represents the voltage-dependent current lost to recombination and I_{sh} represents the shunt resistance current.
Where,

$$I_d = I_s \left[e^{\frac{q \times (V + I_{PV} \times R_s)}{(A \times K \times T)}} - 1 \right] \tag{2}$$

$$I_{sh} = \frac{V + (I_{PV} \times R_s)}{R_{sh}} \tag{3}$$

The light generated current mainly depends on both irradiance and temperature. It is measured on some reference conditions. Thus,

$$I_{ph} = I_{sc} + K_i \times \left(T - T_{ref} \right) \times \frac{\lambda_d}{\lambda_{dref}} \tag{4}$$

where: I_{Ph}—light generated photon current, I_s—cell saturation of dark current, T—cell temperature (Kelvin), T_{ref}—reference temperature (Kelvin), K—Boltzmann's constant (1.38×10^{-23} J/K), q—charge of electron (1.6×10^{-19}°C), K_i—Short circuit current temperature coefficient at I_{sc}, λ_d—solar irradiation (kW/m^2), λ_{dref}—solar irradiation (kW/m^2) at STC—1 kW/m^2, I_{sc}—short circuit current at 25°C, E_g—band gap energy (for silicon, 1.1 eV), A—ideality factor (1.6 for silicon), I_s—cell saturation current at T_{ref}, R_{sh}—shunt resistance (Ω), R_{se}—series resistance (Ω).

To maximize the current and voltage more cells are connected in series parallel. If N_s is the number of cell connected in series and N_p is the number of cell connected in parallel then equation 1 becomes

$$I_{PV} = N_p \times I_{ph} - N_p \times I_s \left(e^{\frac{\frac{V}{N_s} + \frac{I_{PV} \times R_s}{N_s}}{V_t}} - 1 \right) - \left(\frac{V \times N_p}{N_s} + \frac{I_{PV} \times R_s}{R_{sh}} \right) \tag{5}$$

The electricity generated by a photovoltaic module is not only dependent on the irradiance of the sunlight but also the zenith angle θ_z of the sun. Irradiance of the sun (λ_d) on a particular surface of the cell is at its maximum when the cell module and the sun are perpendicular to each other. The irradiance changes with the angle of incident of solar rays. To calculate the energy output of a photo voltaic solar installation an accurate value of solar irradiance needs to be calculated.

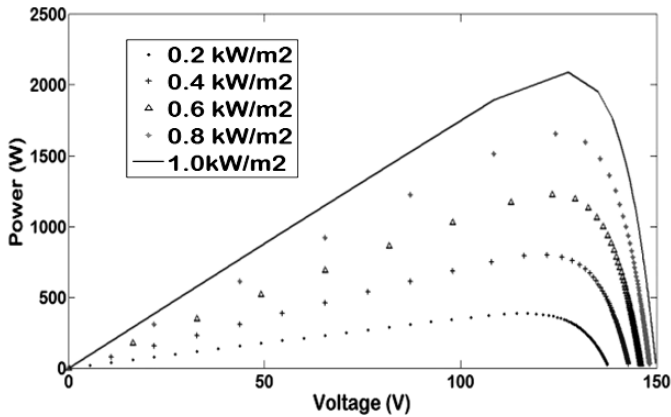$$\lambda_d = 1.353 \times 0.7^{AM^{0.678}} \tag{6}$$
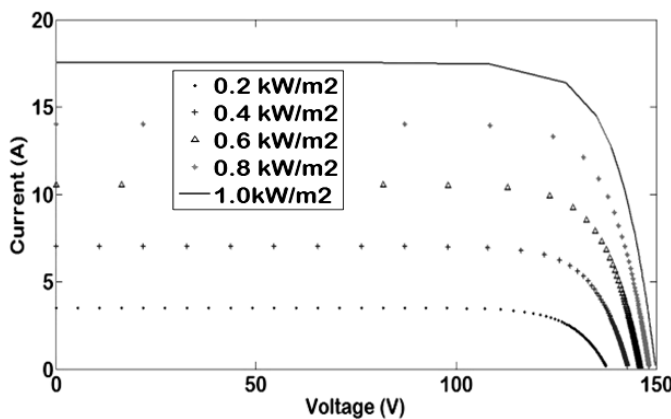
Figure 3: P-V curve of SPV system

Figure 4: I-V curve of SPV system

where

$$AM = \frac{1.003198 \cos \theta_z + 0.101632}{\cos^2 \theta_z + 0.090560 \cos \theta_z + 0.003198} \quad (7)$$

where,

λ_d—solar irradiance perpendicular to the sun kW/m^2, solar constant—1.353 kW/m^2, radiation transmitted to the earth—0.7, AM—sir mass, empirical fit to observed data—0.678, θ_z—zenith angle of the sun.

In this analysis, a solar module (Lanco Solar LSP 250-260M-60) is chosen which provides the required energy to the PMDC motor pump set. For estimation purposes a Simulink model of SPV system is built using the manufacturer data sheet of Lanco Solar LSP 250-260M-60 [15] and the characteristics observed at the different irradiances.

To drive a 2 kW PMDC motor an 8 numbers SPV array is chosen, with 4 numbers SPV arrays connected in series and both connected in parallel to the current requirement according to the PMDC motor full load current requirement. All parameters of the proposed system are based on the 1 kW/m^2 solar irradiance basis, which is the maximum solar irradiance of the sun. As one solar module at STP produces 250–260 W (maximum) so the total power requirement to drive a 2 kW PMDC motor is 8 modules producing 2080 W

(maximum) power. The PV curve and the IV curve of the series parallel combination of the SPV panel is shown in Fig. 3 and Fig. 4 at various irradiances of the Sun where to utilize maximum power in the load section MPPT should be present in the system.

2.2. Maximum Power Point Tracking (MPPT) Controller

There are many MPPT algorithms which are used to extract maximum power from the SPV system. One of them—the perturbation and observation (P&O) method—is used here because it is simple and easy to implement. In the case of the P&O algorithm the operating voltage of the SPV system increments with a smaller value and observes the power extracting by the SPV system. If the extracting power from the SPV system is less than the previous observed power of the SPV, the operating voltage of the SPV system is increased by increasing the duty cycle of the converter, as if the extracting power from the SPV system is greater than the previous observed power of the SPV the operating voltage of the SPV system is decreased by decreasing the duty cycle of the converter. The P&O algorithm is shown in Fig. 5.

2.3. Buck converter

Instead of a boost converter, a Buck converter is utilized to match voltage to the PMDC motor, as is shown in Fig. 6. The switch (MOSFET) is turned on and off continuously and reduces the average output voltage to meet the requirement of the PMDC motor. At the maximum irradiance level of the sun, maximum power is generated by the SPV system at a certain voltage and current level. The Buck converter design is based on the PMDC motor voltage and current requirements at maximum irradiance. The duty cycle may vary automatically or manually.

The output voltage of the Buck converter is

$$V_0 = DV_I \quad (8)$$

where: D is the Duty cycle of the buck converter found from MPPT system, V_I is the generated voltage of the SPV system, V_0 is the output voltage of the buck converter.

The value of the inductor (L) and capacitor (C) is chosen to stabilize the current and voltage ripple.

2.4. Pump Model

Various types of pump (impulse, centrifugal, etc.) are available, to be selected on the basis of head and water discharge per unit. A hydrological investigation determines the head in the area of interest and water discharge depends on the local water demand. The hydrological data and pump efficiency inform the decision on which motor is selected to drive the pump [1]. The power requirements of a pump depend on the pump inlet and outlet pressure, flow rate and density of the fluid. The electrical energy is supplied to the motor, which provides a rotational force to the pump impeller and the rotational force of the impeller extracts water from the underground or surface source [16]. Pump selection is
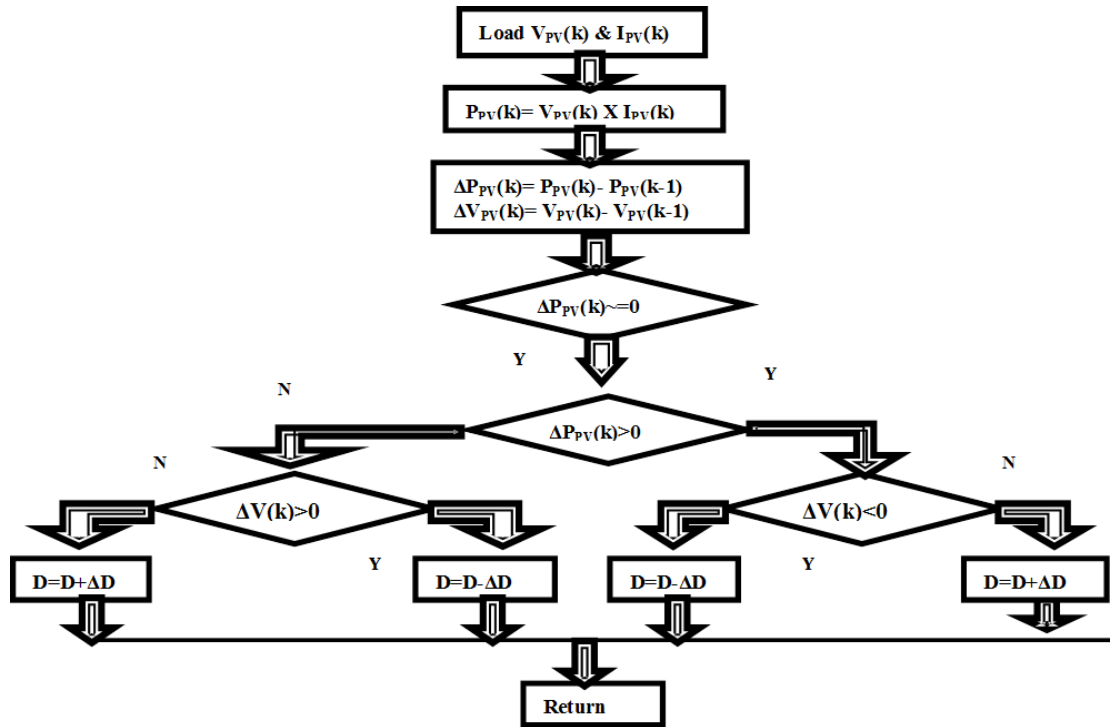
Figure 5: perturbation and observation (P&O) algorithm for MPPT controller
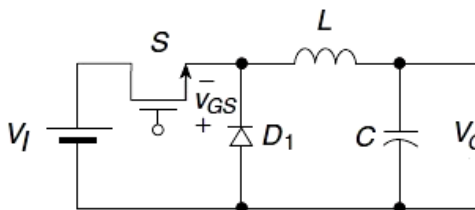

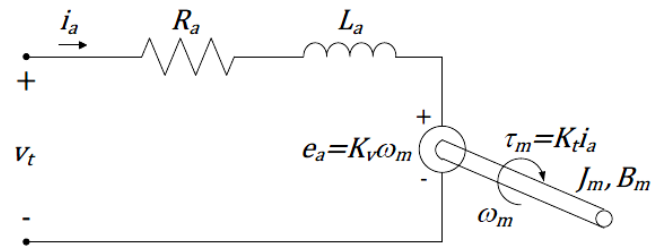Figure 6: Buck converter connected with LC filter and resistive load

Figure 7: Simplified PMDC motor model

not included in this section, which contains a general investigation into the centrifugal pump, which is very useful for medium head and surface water pumping.

To investigate the performance of a centrifugal pump, the pump impeller is connected to the shaft of a 2 kW PMDC motor shaft. The load torque (T_L) attached to the motor for the centrifugal pump load depends on the rotor speed (ω_m) which is shown below [11].

$$T_L = T_L(\omega_m) = T_{L0} + T_{L1}\omega_m + T_{L2}\omega_m^2 \qquad (9)$$

where $T_{L0} = 1.217e^{-5}$, $T_{L1} = 9.917e^{-5}$, $T_{L2} = 5.939e^{-5}$.

2.5. PMDC motor

A permanent magnet DC motor (PMDC) consists of a stator, rotor and a commutator, whereas the brush is like a conventional DC motor where the field coil is replaced by a permanent magnet. The advantage of the PMDC motor over the traditional DC motor is the simple connection and smooth speed control by changing the armature voltage. The only

disadvantage related to the PMDC motor is that its field is constant, so the flux control method of speed control is not possible here [17]. The stator of the motor is made of ferrite material, which provides adequate flux for excitation of the PMDC motor. The rotating part where emf is induced is called the armature of the PMDC motor and is directly connected to the DC supply using a commutator brush arrangement.

The mathematical model [18] of the PMDC motor shown below can be represented by the differential equation derived from Kirchhoff's voltage law and Newton's law of motion applied in a rotational system, as is shown in Fig. 7.

Whenever a voltage has been applied to the motor, the torque developed at the shaft of the PMDC motor is given by the following equation:

$$\tau_m = k_t i_a \qquad (10)$$

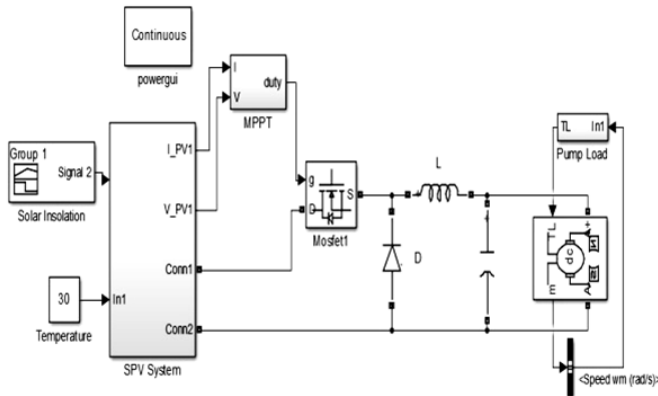The electrical characteristics of PMDC motor are shown in

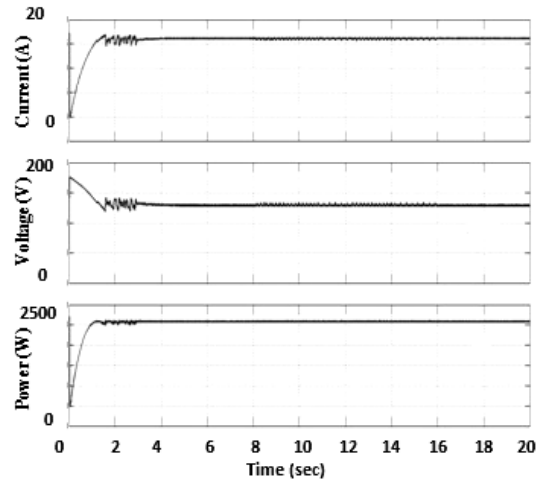Figure 8: MPPT connected Solar SPV connected PMDC pump

Figure 9: MPPT connected SPV system Current (A), Voltage (V) and power (W) characteristics with respect to time at irradiance 1 kW/m^2

equation no (11)

$$v_t = R_a I_a + L_a \frac{di_a}{dt} + e_a \qquad (11)$$

where $e_a = k_v \omega_m$.

The developed torque produces speed ω_m, which relates to the inertia and damping friction of the motor. The mechanical characteristics of the PMDC motor are shown in equation no (12)

$$k_t i_a - J_m \frac{d\omega_m}{dt} - B_m \omega_m - T_L = 0 \qquad (12)$$

where: ω_m—motor Torque, R_a is the armature resistance, L_a is the inductance of the armature, v_t is the terminal voltage, I_a is the current of the motor, e_a is the induced voltage or back emf induced by the rotation of the armature, J_m—the motor inertia, B_m—damping friction of the motor and T_L is the motor load.

The above equation represents the mathematical model of the PMDC motor which is formulated using MATLAB/Simulink software and investigates the characteristics of the SPV connected PMDC motor.

Here, a 2 kW PMDC motor has been chosen for analysis and performance of the PMDC motor under various levels of irradiance of the sun. It is investigated for a directly connected SPV-PMDC motor system and an MPPT connected SPV-PMDC motor system.

3. Results and discussion

The analysis was carried out in the MATLAB/Simulink environment, which is shown in Fig. 8. For simplicity the temperature of the SPV system is kept constant and the characteristics of the SPV connected PMDC were investigated for both high irradiance (1 kW/m^2) and low irradiance (0.3 kW/m^2). The results obtained from the MPPT connected SPV-PMDC system were compared with the directly connected SPV-PMDC system and demonstrate the superiority of the MPPT connected SPV-PMDC system over the directly connected SPV-PMDC system. The operation of the centrifugal pump depends on the speed of the PMDC motor, hence for better water pumping, the speed of the motor should be constant and the energy utilization of the PMDC motor should be at a maximum in all conditions from low to high solar irradiance. Fig. 8 shows the overall MPPT controller connected Solar SPV-PMDC pump system.

At maximum irradiance (irradiance = 1 kW/m^2) the MPPT controller connected SPV system voltage & current and power generation and power utilized by the PMDC motor is shown in Fig. 9.

At 1 kW/m^2 irradiance the MPPT connected SPV generates power of around 2087 W at a voltage of 146 V and a current of 13.5 A is at the maximum level of voltage and current and stable and is desirable for the PMDC connected centrifugal pump. The I-V and P-V characteristics of the MPPT controller connected SPV system is shown in Fig. 10a and Fig. 10b.

Fig. 10a and Fig. 10b shows that at maximum irradiance (1 kW/m^2) the MPPT controller sets the operating voltage at maximum power by changing the duty cycle of the chopper. As the operating voltage of the PMDC motor is in the maximum power zone, the energy utilized by the PMDC motor is also at maximum—which is desirable for overall efficiency of the system. The only problem with the MPPT controller is that the voltage and current profile experiences some oscillation, because of the continuous change of duty cycle of the chopper; and the operating voltage and currents also oscillate. The output voltage and current profile of the step down chopper is shown in Fig. 11 where an L-C filter is applied to reduce the oscillation of the voltage and current profile within limits.

The generated energy of SPV system and the utilized energy by the PMDC pump are shown in Fig. 11. The energy drawn from the SPV system by the PMDC motor is around 1979.64 W at a voltage of 99.63 V and operating current of 19.87 A is within the specified rating of the motor. Efficiency is high and the oscillation dependent on the continu-
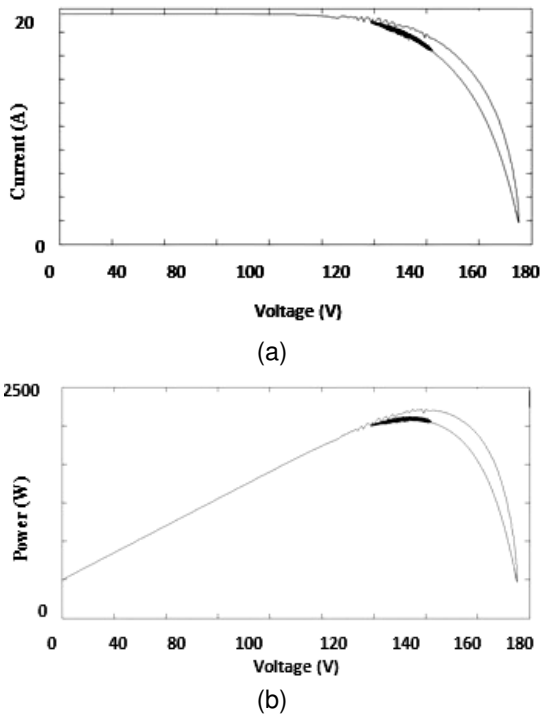
(a)

(b)

Figure 10: I-V characteristics of SPV array at 1 kW/m^{2}solar irradiance (a), P-V characteristics of SPV array at 1 kW/m^{2}solar irradiance (b)

Figure 11: Chopper voltage (V_Ch) and current (I_Ch) and Power generated by MPPT connected SPV (P_PV) and utilized by PMDC (P_PMDC) profile for MPPT connected SPV system at irradiance 1 kW/m^2

Figure 12: PMDC speed (ω_m), current (i_A) electromagnetic torque (T_e) and load torque (T_L) characteristic at MPPT connected SPV system at irradiance 1 kW/m^2

ous change of duty cycle is reduced by the L-C filter circuit which is attached to the step down chopper.

For a centrifugal pump the water flow rate is proportional to the speed of the motor for constant head operation. The characteristics of the PMDC motor show it rotates at a speed of 115.65 rad/sec (1105 rpm) and the speed profile is stable, and hence pumping operation is satisfactory in the case of the MPPT connected SPV-PMDC motor connected system shown in Fig. 12.

The above experiment is then carried out using the directly connected SPV system. The duty cycle 0.71 is chosen as per the maximum voltage generated by the SPV system and matches the nameplate data of the PMDC motor.

At maximum irradiance (irradiance = 1 kW/m^2) the directly connected SPV system voltage & current and power generation by the PMDC motor are shown in Fig. 13.

The SPV system generates around 1983 W power at a voltage of 146 V and 13.5 A current lying in the maximum region at irradiance = 1 kW/m^2. The chopper circuit reduced the voltage generated to 96.33 V and the current of around 18.73 A is within the region of the PMDC motor nameplate data. As the duty cycle of the chopper circuit is constant, the oscillation of the voltage and current profile is very low and L-C filter size is very small compared to the MPPT connected SPV PMDC system. The chopper characteristics and energy utilization by the PMDC motor are shown in Fig. 14.

At high irradiance (irradiance = 1 kW/m^2) the voltage and current profile are at a maximum and stable. Hence the PMDC motor speed of around 112.20 rad/sec (1072 rpm) is also constant, as is shown in Fig. 15.
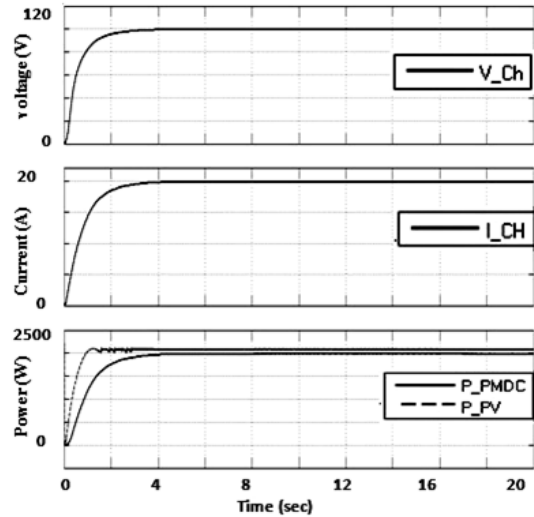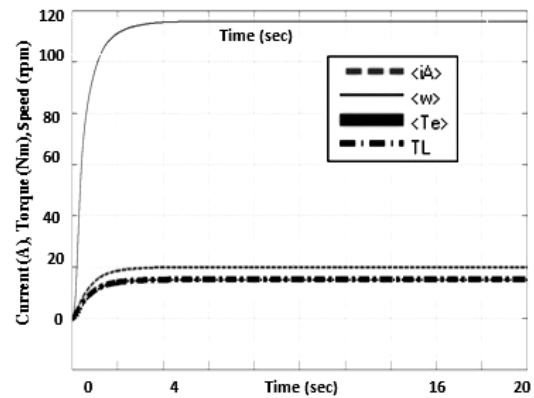
The above experiment is then repeated at low irradiance (irradiance = 0.3 kW/m^2) to investigate the superiority of the MPPT controller connected SPV system over the directly connected SPV system. The MPPT connected SPV system generates 614.4 W power at a voltage level of around 128 V and current of around 4.8 A. At low irradiance the I-V and P-V characteristics of the directly connected SPV and MPPT connected SPV are shown in Fig. 16.

The I-V and P-V characteristics indicate that at low irradiance (0.3 kW/m)^2) the MPPT controller works properly and the operating voltage is in the maximum power region.

The chopper voltage, current profile and the comparison of energy utilized by the PMDC motor are shown in Fig. 17 and the PMDC characteristics profile is shown in Fig. 18. At low irradiance too much variation of the duty cycle generates oscillating voltage and currents in the SPV system, which has to be damped out at the chopper end. The filter connected at the chopper end damps out the oscillation and stabilizes
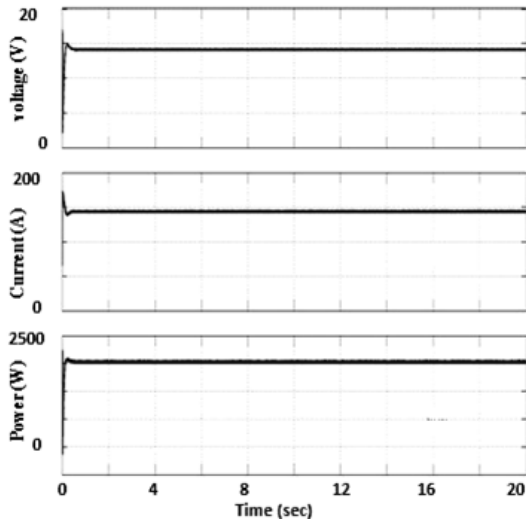
Figure 13: Directly connected SPV Current (A), Voltage (V) and power (W) characteristics with respect to time at irradiance 1 kW/m^2
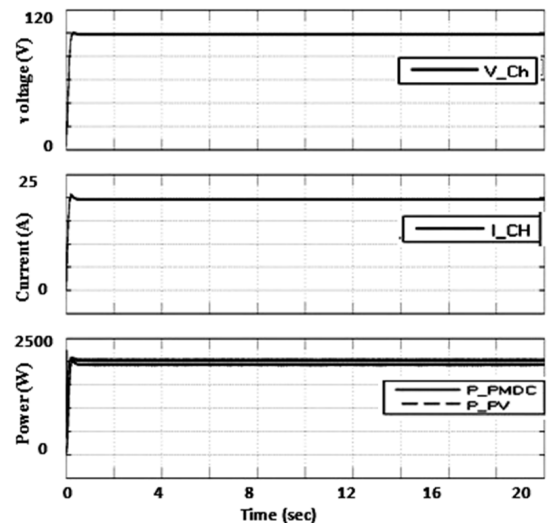

Figure 14: Step down chopper voltage (V_Ch) and current (I_Ch) and Power generated by SPV (P_PV) and utilized by PMDC (P_PMDC) profile for directly connected SPV system at irradiance 1 kW/m^2

the generated voltage at 63.38 V and current around 8.75 A. Fig. 18 shows the PMDC motor speed profile. The PMDC motor rotates at an almost constant speed of 76.30 rad/sec (729 rpm). Hence the operation of the pump is also satisfactory at low irradiance.

The performance of the directly connected SPV system at the same irradiance (0.3 kW/m^2) is also investigated in this section.

Fig. 19 shows the energy utilization of the PMDC motor from a directly connected SPV system. The SPV generated power is fluctuating at the initial stage, which is not suitable for PMDC motor connected pump operation, and stabilizes within a few seconds; the stable operating voltage is around 56.8 V and stable operating current is around 7.193 A. The energy utilized by the PMDC motor is around 408.56 W, which is low compared to the MPPT connected SPV system, where the power drawn by the PMDC motor is 554.57 W at the same irradiance of 0.3 kW/m^2.

Fig. 20 indicates the PMDC motor characteristics at a directly connected SPV system where the PMDC motor oscillates in the initial stages and stabilizes within a few seconds at a speed of around 69.2 rad/sec (661.2 rpm). The lower speed indicates lower water extraction compared to the MPPT connected SPV system at low irradiance.

From Fig. 20 it is evident that for the MPPT connected SPV-PMDC system (compared to the directly connected SPV-PMDC system) the PMDC motor utilizes maximum power in the case of the MPPT connected system and the motor characteristics also show a better result and hence the performance of the centrifugal pump also improves.

4. Conclusions

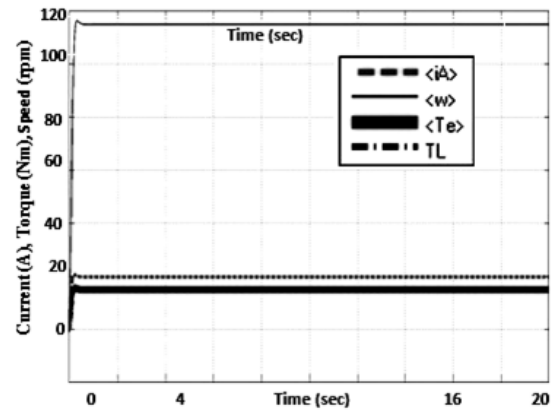In this paper a comparison is made between the directly connected SPV pumping system and the MPPT controller

Figure 15: PMDC speed (ω_m), current (i_A) electromagnetic torque (T_e) and load torque (T_L) characteristics for the directly connected SPV system at irradiance 1 kW/m^2

connected SPV pumping system, and investigated. For simplicity the temperature of the environment is kept constant and the water pumping operation of the PMDC motor and centrifugal pump considered. At high irradiance (irradiance 1 kW/m^2) the energy utilized by the PMDC motor is 8.8% higher in the case of the MPPT connected SPV water pumping system compared to the directly connected SPV system and the rotational speed is also 2% higher than the latter. At low irradiance (irradiance 0.3 kW/m^2) the energy utilization by the PMDC motor is 26% higher in the case of the MPPT connected SPV system than the directly connected SPV system, and at low irradiance the speed of the PMDC motor is 9.3% higher than the latter. At low irradiance the voltage and current oscillate and a suitable filter circuit has to be implemented with a chopper circuit to stabilize the operating voltage and current profile. At both high and low irradiance the MPPT controller connected SPV with PMDC motor pump system performs with higher overall efficiency than the
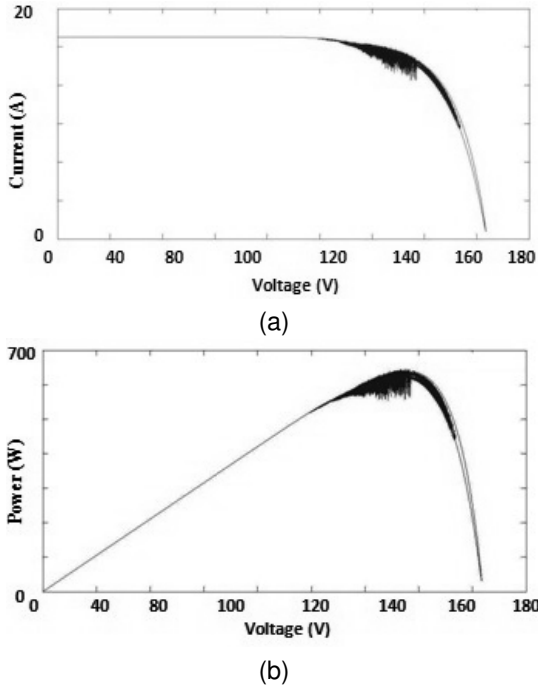
(a)

(b)

Figure 16: I-V characteristics of SPV array at 0.3 kW/m^2 solar irradiance (a), P-V characteristics of SPV array at 0.3 kW/m^2 solar irradiance (b)

directly connected SPV with PMDC motor pump system.

Figure 17: Chopper voltage (V_Ch) and current (I_Ch) and Power generated by MPPT connected SPV (P_PV) and utilized by PMDC (P_PMDC) profile for MPPT connected SPV system at irradiance 0.3 kW/m^2

Figure 18: PMDC speed (ω_m), current (i_A) electromagnetic torque (T_e) and load torque (T_L) characteristics of MPPT connected SPV system at irradiance 0.3 kW/m^2

References

[1] N. Argaw, R. Foster, A. Ellis, Renewable energy for water pumping applications in rural villages; period of performance: April 1, 2001–september 1, 2001, Tech. rep., National Renewable Energy Laboratory (NREL), Golden, CO. (2003).

[2] A. Mokeddem, A. Midoun, N. Ziani, D. Kadri, S. Hiadsi, Test and analysis of a photovoltaic dc-motor pumping system, in: ICTON Mediterranean Winter Conference, 2007. ICTON-MW 2007, IEEE, 2007, pp. 1–7.

[3] M. A. Vitorino, M. B. R. Corrêa, High performance photovoltaic pumping system using induction motor, in: Power Electronics Conference, 2009. COBEP'09. Brazilian, IEEE, 2009, pp. 797–804.

[4] F. Zebiri, A. Kessal, L. Rahmani, A. Chebabhi, Analysis and design of photovoltaic pumping system based on nonlinear speed controller, Journal of Power Technologies 96 (1) (2016) 40–48.

[5] N. Chandrasekaran, G. Ganeshprabu, K. Thyagarajah, Comparative study of photovoltaic pumping system using a dc motor and pmdc motor, in: Advances in Engineering, Science and Management (ICAESM), 2012 International Conference on, IEEE, 2012, pp. 129–132.
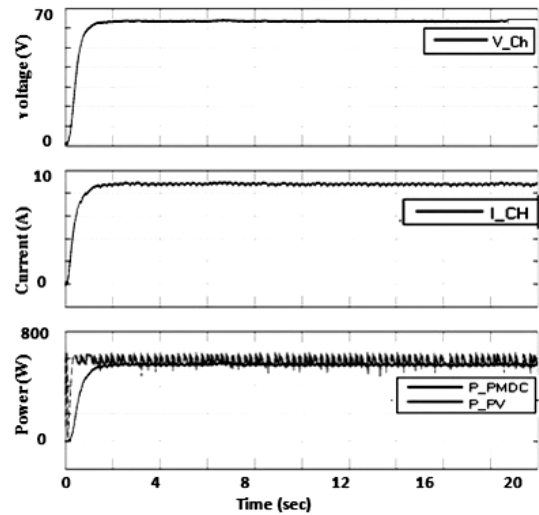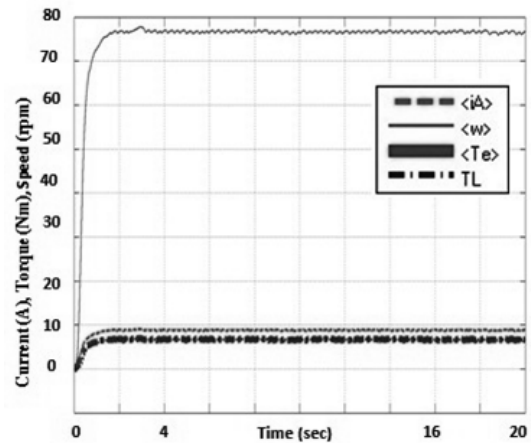
[6] N. B. Yousuf, K. M. Salim, R. Haider, M. R. Alam, F. B. Zia, Development of a three phase induction motor controller for solar powered water pump, in: Developments in Renewable Energy Technology (IC-DRET), 2012 2nd International Conference on the, IEEE, 2012, pp. 1–5.

[7] B. Singh, A. K. Mishra, R. Kumar, Solar powered water pumping system employing switched reluctance motor drive, IEEE Transactions on Industry Applications 52 (5) (2016) 3949–3957.

[8] R. Kumar, B. Singh, Solar photovoltaic array fed canonical switching cell converter based bldc motor drive for water pumping system, in: India Conference (INDICON), 2014 Annual IEEE, IEEE, 2014, pp. 1–6.

[9] H. M. Karkar, S. N. Pandya, V/F method for induction motor drive speed control using matlab simulation, Journal of Information Knowledge and Research in Electrical Engineering 2 (2) (2014) 192–197.

[10] P. Krause, O. Wasynczuk, S. D. Sudhoff, S. Pekarek, Analysis of electric machinery and drive systems, Vol. 75, John Wiley & Sons, 2013.

[11] N. Rebei, R. Gammoudi, A. Hmidet, O. Hasnaoui, Experimental implementation techniques of p&o mppt algorithm for pv pumping system, in: Systems, Signals & Devices (SSD), 2014 11th International Multi-Conference on, IEEE, 2014, pp. 1–6.
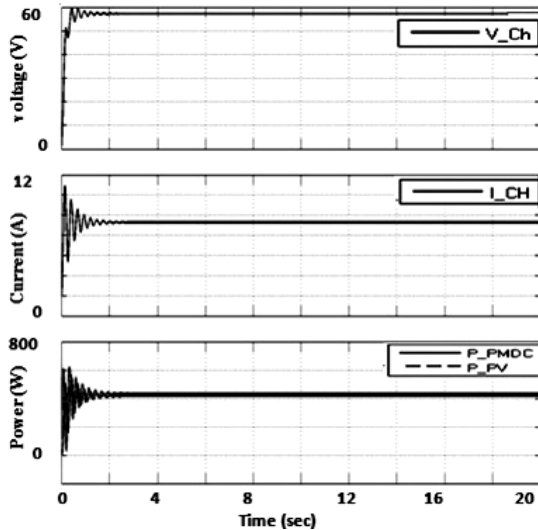
(2013) 39–57.

Figure 19: Chopper voltage (V_Ch) and current (I_Ch) and Power generated by MPPT connected SPV (P_PV) and utilized by PMDC (P_PMDC) profile for directly connected SPV system at irradiance 0.3 kW/m^2
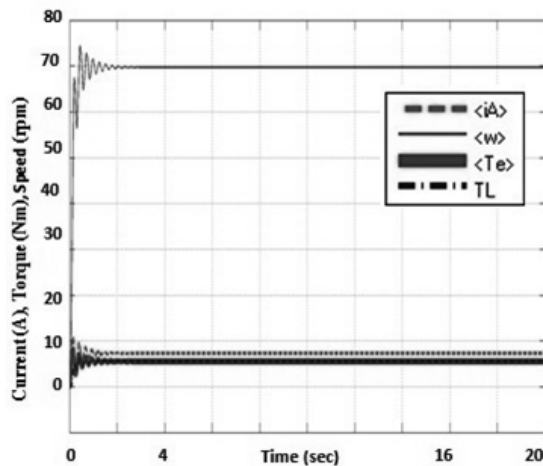

Figure 20: PMDC speed (ω_m), current (i_A) electromagnetic torque (T_e) and load torque (T_L) characteristics at directly connected SPV system at irradiance 0.3 kW/m^2

[12] M. G. Villalva, J. R. Gazoli, E. Ruppert Filho, Comprehensive approach to modeling and simulation of photovoltaic arrays, IEEE Transactions on power electronics 24 (5) (2009) 1198–1208.

[13] A. El Shahat, PV module optimum operation modeling, Journal of Power technologies 94 (1) (2014) 50–66.

[14] R. Schoenmaker, Developing a smart grid simulation model from an end-users perspective, Master's thesis, Vniversity of Groningen, Groningen (January 2014).

[15] S. Sharma, R. Raman, K. Kaja, High efficiency lanco solar pv mono crystalline modules, Lanco Solar Pvt. Limited.
URL http://www.lancosolar.com

[16] J. Milewski, M. Wolowicz, W. Bujalski, Methodology for choosing the optimum architecture of a stes system, Journal of Power Technologies 94 (3) (2014) 153–164.

[17] S. Chapman, Electric machinery fundamentals, Tata McGraw-Hill Education, 2005.

[18] A. A. Mahfouz, M. Mohammed, F. A. Salem, Modeling, simulation and dynamics analysis issues of electric motor, for mechatronics applications, using different approaches and verification by matlab/simulink, International Journal of Intelligent Systems and Applications 5 (5)